

A Mean-Variance Objective for Robust Production Optimization in Uncertain Geological Scenarios

Andrea Capolei^a, Eka Suwartadi^b, Bjarne Foss^b, John Bagterp Jørgensen^{a,*}

^a*Department of Applied Mathematics and Computer Science & Center for Energy Resources Engineering
Technical University of Denmark, DK-2800 Kgs. Lyngby, Denmark.*

^b*Department of Engineering Cybernetics, Norwegian University of Science and Technology (NTNU), 7491 Trondheim, Norway.*

Abstract

In this paper, we introduce a mean-variance criterion for production optimization of oil reservoirs and suggest the Sharpe ratio as a systematic procedure to optimally trade-off risk and return. We demonstrate by open-loop simulations of a two-phase synthetic oil field that the mean-variance criterion is able to mitigate the significant inherent geological uncertainties better than the alternative certainty equivalence and robust optimization strategies that have been suggested for production optimization. In production optimization, the optimal water injection profiles and the production borehole pressures are computed by solution of an optimal control problem that maximizes a financial measure such as the Net Present Value (NPV). The NPV is a stochastic variable as the reservoir parameters, such as the permeability field, are stochastic. In certainty equivalence optimization, the mean value of the permeability field is used in the maximization of the NPV of the reservoir over its lifetime. This approach neglects the significant uncertainty in the NPV. Robust optimization maximizes the expected NPV over an ensemble of permeability fields to overcome this shortcoming of certainty equivalence optimization. Robust optimization reduces the risk compared to certainty equivalence optimization because it considers an ensemble of permeability fields instead of just the mean permeability field. This is an indirect mechanism for risk mitigation as the risk does not enter the objective function directly. In the mean-variance bi-criterion objective function risk appears directly, it also considers an ensemble of reservoir models, and has robust optimization as a special extreme case. The mean-variance objective is common for portfolio optimization problems in finance. The Markowitz portfolio optimization problem is the original and simplest example of a mean-variance criterion for mitigating risk. Risk is mitigated in oil production by including both the expected NPV (mean of NPV) and the risk (variance of NPV) for the ensemble of possible reservoir models. With the inclusion of the risk in the objective function, the Sharpe ratio can be used to compute the optimal water injection and production borehole pressure trajectories that give the optimal return-risk ratio. By simulation, we investigate and compare the performance of production optimization by mean-variance optimization, robust optimization, certainty equivalence optimization, and the reactive strategy. The optimization strategies are simulated in open-loop without feedback while the reactive strategy is based on feedback. The simulations demonstrate that certainty equivalence optimization and robust optimization are risky strategies. At the same computational effort as robust optimization, mean-variance optimization is able to reduce risk significantly at the cost of slightly smaller return. In this way, mean-variance optimization is a powerful tool for risk management and uncertainty mitigation in production optimization.

Keywords: Robust Optimization, Risk Management, Oil Production, Optimal Control, Mean-Variance Optimization, Uncertainty Quantification

1. Introduction

In conventional water flooding of an oil field, feedback based optimal control technologies may enable higher oil recovery than with a conventional reactive strategy in which producers are closed based on water breakthrough (Chierici, 1992; Ramirez, 1987).

Optimal control technology and Nonlinear Model Predictive Control (NMPC) have been suggested for improving the oil recovery during the water flooding phase of an oil field (Jansen

et al., 2008). In such applications, the controller adjusts the water injection rates and the bottom hole well pressures to maximize oil recovery or a financial measure such as the NPV. In the oil industry, this control concept is also known as closed-loop reservoir management (CLRM) (Foss, 2012; Jansen et al., 2009). The controller in CLRM consists of a state estimator for history matching (state and parameter estimation) and an optimizer that solves a constrained optimal control problem for the production optimization. Each time new measurements from the real or simulated reservoir are available, the state estimator uses these measurements to update the reservoir's models and the optimizer solves an open loop optimization problem with the updated models (Capolei et al., 2013). Only the first part of the resulting optimal control trajectory is implemented. As new

*Corresponding author

Email addresses: acap@dtu.dk (Andrea Capolei), eka.suwartadi@ieee.org (Eka Suwartadi), Bjarne.Foss@itk.ntnu.no (Bjarne Foss), jbj@dtu.dk (John Bagterp Jørgensen)

measurements become available, the procedure is repeated. The main difference of the CLRM system from a traditional NMPC is the large state dimension (10^6 is not unusual) of an oil reservoir model (Binder et al., 2001). The size of the problem dictates that the ensemble Kalman filter is used for state and parameter estimation (history matching) and that single shooting optimization is used for computing the solution of the optimal control problem (Capolei et al., 2013; Jansen, 2011; Jørgensen, 2007; Sarma et al., 2005a; Suwartadi et al., 2012; Völcker et al., 2011).

In this paper, we focus on the formulation of the optimization problem in the NMPC for CLRM. In the study of different optimization formulations, we leave out data assimilation (history matching) as well as the effect of feedback from a moving horizon implementation and consider only the predictions and computations of the manipulated variables in the open-loop optimization of NMPC. This can be regarded as an optimal control study. The reason for this is twofold. First, in the initial development of a field, no production data would be available and the production optimization would be an open-loop optimal control problem, i.e. without feedback from measurements. Secondly, the ability of different optimization strategies to mitigate the effect of the significant uncertainties present in reservoir models is better understood if investigated in isolation.

In conventional production optimization, the nominal net present value (NPV) of the oil reservoir is maximized (Brouwer and Jansen, 2004; Capolei et al., 2013, 2012b; Foss, 2012; Foss and Jensen, 2011; Nævdal et al., 2006; Sarma et al., 2005b; Suwartadi et al., 2012). To compute the nominal NPV, nominal values for the model's parameters are used. In certainty equivalence production optimization, the expected reservoir model parameters are used in the maximization, while robust production optimization uses an ensemble of reservoir models to maximize the expected NPV (Capolei et al., 2013; Van Essen et al., 2009). Certainty equivalence optimization is equivalent to robust optimization for the ideal case of unconstrained linear dynamics with Gaussian additive noise and quadratic cost functions, i.e. for Linear Quadratic Gaussian (LQG) problems (Bertsekas, 2005; Stengel, 1994). For all other problems, the certainty equivalence optimization and the robust optimization are different. Both certainty equivalence optimization and robust optimization assume that the stochastic event is repeated infinitely many times such that only the expected value but not the risk is of interest. The purpose of the robust production optimization is to (indirectly) mitigate the effect of the significant uncertainties in the parameters of the reservoir model. However, by the certainty equivalence and the robust production optimization methods, the trade-off between return (expected NPV) and risk (variance of the NPV) is not addressed directly. Fig. 1 illustrates risk versus expected return (mean) for different optimization and operation strategies. This is a sketch that shows the qualitative behavior of the results in this paper. As is evident in the sketch, a significant risk is typically associated with the certainty equivalence optimization and the RO strategy. The implication is that the RO strategy may improve current operation, but you cannot be sure due to the significant risk arising from the uncertain reservoir model. This is prob-

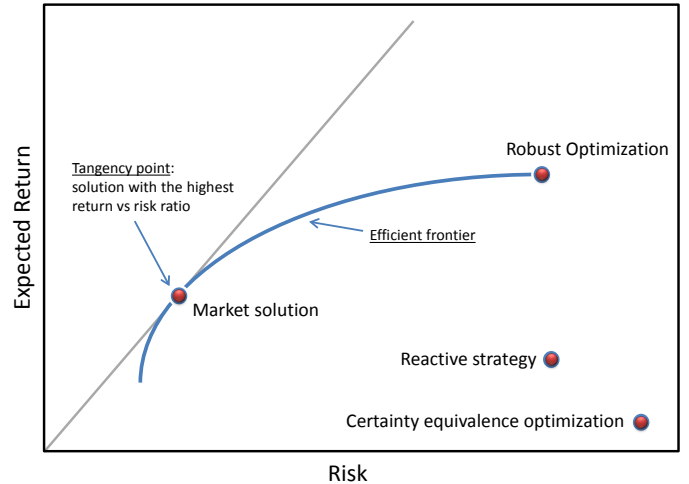


Figure 1: A sketch of the trade-off between risk and expected return in different optimization methods implemented in the optimizer for model based production optimization.

ably one of the reasons that NMPC for CLRM has not been widely adopted in the operation of oil reservoirs. The optimization problem in production optimization can be compared in some sense to Markowitz portfolio optimization problem in finance (Markowitz, 1952; Steinbach, 2001) or to robust design in topology optimization (Beyer and Sendhoff, 2007; Lazarov et al., 2012). The key to mitigate risk is to optimize a bi-criterion objective function including both return and risk for the ensemble of possible reservoir models. In this way, we can use a single parameter to compute an efficient frontier (the blue Pareto curve in Fig. 1) of risk and expected return. The robust optimization is one limit of the efficient frontier and the other limit is the minimum risk minimum return solution. By proper balancing the risk and the return in the bi-criterion objective function, we can tune the optimizer in the controller such that an optimal ratio of return vs risk is obtained; such a solution is called the market solution and is illustrated in Fig. 1.

The mean-variance optimization is based on a bi-criterion objective function. Previously in the oil literature, multi-objective functions have been used in production optimization to trade-off long- and short-term NPV (Van Essen et al., 2011), to robustify a non-economic objective function (Alhuthali et al., 2008), and to trade-off oil production, water production and water injection using a combination of mean value and standard deviation for each term (Yasari et al., 2013). These approaches pointed to the fact that a multi-objective function may be used to trade-off risk for performance, but did not explicitly address the risk-return relationship studied in the present paper using a mean-variance optimization strategy. Furthermore, these papers did not provide a systematic method for selection of the risk adverse parameter. The main contribution of the present paper is to demonstrate, that a return-risk bi-criterion objective function is a valuable tool for the profit-risk trade-off and provide a systematic method for selection the risk-return trade-off parameter. We do this for the open loop optimization and do not consider the effect of feedback.

The paper is organized as follows. Section 2 defines the reservoir model. Section 3 states the constrained optimal control problem and describes the mean-variance optimization strategy. The computation of economical and production key performance indicators is explained in Section 4. Section 5 describes the numerical case study. Conclusions are presented in Section 6.

2. Reservoir Model

We assume that the reservoirs are in the secondary recovery phase where the pressures are above the bubble point pressure of the oil phase. Therefore, two-phase immiscible flow, i.e. flow without mass transfer between the two phases, is a reasonable assumption. We focus on water-flooding cases for two-phase (oil and water) reservoirs. Further, we assume incompressible fluids and rocks, no gravity effects or capillary pressure, no-flow boundaries, and isothermal conditions. The state equations in an oil reservoir Ω , with boundary $\partial\Omega$ and outward facing normal vector \mathbf{n} , can be represented by pressure and saturation equations. The pressure equation is described as

$$\mathbf{v} = -\lambda_t \mathbf{K} \nabla p, \quad \nabla \cdot \mathbf{v} = \sum_{i \in \mathcal{I}, \mathcal{P}} q_i \cdot \delta(\mathbf{r} - \mathbf{r}_i) \quad \mathbf{r} \in \Omega \quad (1a)$$

$$\mathbf{v} \cdot \mathbf{n} = 0 \quad \mathbf{r} \in \partial\Omega \quad (1b)$$

\mathbf{r} is the position vector, \mathbf{r}_i is the well position, \mathbf{v} is the Darcy velocity (total velocity), \mathbf{K} is the permeability, p is the pressure, q_i is the volumetric well rate in barrels/day, δ is the Dirac's delta function, \mathcal{I} is the set of injectors, \mathcal{P} is the set of producers, and λ_t is the total mobility. The total mobility, λ_t , is the sum of the water and oil mobility functions

$$\lambda_t = \lambda_w(s) + \lambda_o(s) = k_{rw}(s)/\mu_w + k_{ro}(s)/\mu_o \quad (2)$$

The saturation equation is given by

$$\phi \frac{\partial}{\partial t} S_w + \nabla \cdot (f_w(S_w) \mathbf{v}) = \sum_{i \in \mathcal{I}, \mathcal{P}} q_{w,i} \cdot \delta(\mathbf{r} - \mathbf{r}_i) \quad (3)$$

ϕ is the porosity, s is the saturation, $f_w(s)$ is the water fractional flow which is defined as $\frac{\lambda_w}{\lambda_t}$, and $q_{w,i}$ is the volumetric water rate at well i . We use the MRST reservoir simulator to solve the pressure and saturation equations, (1) and (3), sequentially (Lie et al., 2012). Specifically, MRST first computes the total mobility using the initial water saturation. Secondly, the pressure equation is solved explicitly using the initial water saturation and the computed total mobility value. Thirdly, with the obtained pressure solution, the velocity is computed and is used in an implicit Euler method to solve the saturation equation. This procedure is repeated until the final time is reached. Wells are implemented using the Peaceman well model (Peaceman, 1983)

$$q_i = -\lambda_t W I_i (p_i - p_i^{bhp}) \quad (4)$$

p_i^{BHP} is the wellbore pressure, and $W I_i$ is the Peaceman well-index. The volumetric water flow rates at injection and production wells are

$$q_{w,i} = q_i \quad i \in \mathcal{I} \quad (5a)$$

$$q_{w,i} = f_w q_i \quad i \in \mathcal{P} \quad (5b)$$

The volumetric oil flow rates at production wells are

$$q_{o,i} = (1 - f_w) q_i \quad i \in \mathcal{P} \quad (6)$$

3. Optimal Control Problem

In this section, we present the continuous-time constrained optimal control problem and its transcription by the single shooting method to a finite dimensional constrained optimization problem. First we present the continuous-time optimal control problem; then we parameterize the control function using piecewise constant basis functions; and finally we convert the problem into a constrained optimization problem using the single shooting method.

Consider the continuous-time constrained optimal control problem in the Lagrange form

$$\max_{x(t), u(t)} J = \int_{t_a}^{t_b} \Phi(x(t), u(t)) dt \quad (7a)$$

subject to

$$x(t_a) = x_0, \quad (7b)$$

$$\frac{d}{dt} g(x(t)) = f(x(t), u(t), \theta), \quad t \in [t_a, t_b], \quad (7c)$$

$$u(t) \in \mathcal{U}(t). \quad (7d)$$

$x(t) \in \mathbb{R}^{n_x}$ is the state vector, $u(t) \in \mathbb{R}^{n_u}$ is the control vector, and θ is a parameter vector in an uncertain space Θ (in our case the permeability field). The time interval $I = [t_a, t_b]$ as well as the initial state, x_0 , are assumed to be fixed. (7c) represents the dynamic model and includes systems described by index-1 differential algebraic equations (DAE) (Capolei et al., 2012a,b; Völcker et al., 2009). (7d) represents linear bounds on the input values, e.g. $u_{\min} \leq u(t) \leq u_{\max}$. In our formulations we do not allow nonlinear state or output constraints. Suwartadi et al. (2012) provide a discussion of output constraints.

3.1. Production Optimization

Production optimization aims at maximizing the net present value (NPV) or the oil recovery for the life time of the oil reservoir. The stage cost, Φ , in the objective function for a NPV maximization can be expressed as

$$\Phi(x(t), u(t)) = \frac{-1}{(1 + \frac{d}{365})^{\tau(t)}} \left[\sum_{i \in \mathcal{I}} r_{wi} q_i(u(t), x(t)) + \sum_{i \in \mathcal{P}} (r_o q_{o,i}(u(t), x(t)) - r_{wp} q_{w,i}(u(t), x(t))) \right] \quad (8)$$

r_o , r_{wp} , and r_{wi} represent the oil price, the water separation cost, and the water injection cost, respectively. $q_{w,i}$ and $q_{o,i}$ are the volumetric water and oil flow rate at producer i ; q_l is the volumetric well injection rate at injector l ; d is the annual interest rate and $\tau(t)$ is the integer number of days at time t . The discount factor $(1 + \frac{d}{365})^{-\tau(t)}$ accounts for a daily compounded value of the capital. Note that from the well model (4), it follows that the flow rates, q , are negative for the producer wells and positive for the injector wells. Hence, the negative sign in front of the square bracket in the stage cost, Φ . Note that in the special case when the discount factor is zero ($d = 0$) and the water injection and separation costs are zero as well, the NPV is equivalent to the quantity of produced oil.

3.2. Control Vector Parametrization

Let T_s denote the sample time such that an equidistant mesh can be defined as

$$t_a = t_0 < \dots < t_S < \dots < t_N = t_b \quad (9)$$

with $t_j = t_a + jT_s$ for $j = 0, 1, \dots, N$. We use a piecewise constant representation of the control function in this equidistant mesh, i.e. we approximate the control vector in every subinterval $[t_j, t_{j+1}]$ by the zero-order-hold parametrization

$$u(t) = u_j, u_j \in \mathbb{R}^{n_u}, t_j \leq t < t_{j+1}, j \in 0, \dots, N-1 \quad (10)$$

The optimizer maximizes the net present value by manipulating the well bhp. A common alternative is to use the injection rates as manipulated variables (Capolei et al., 2012b). The manipulated variables at time period $k \in \mathcal{N}$ are $u_k = \{\{p_{i,k}^{bhp}\}_{i \in \mathcal{I}}, \{p_{i,k}^{bhp}\}_{i \in \mathcal{P}}\}$ with \mathcal{I} being the set of injectors and \mathcal{P} being the set of producers. For $i \in \mathcal{I}$, $p_{i,k}^{bhp}$ is the bhp (bar) in time period $k \in \mathcal{N}$ at injector i . For $i \in \mathcal{P}$, $p_{i,k}^{bhp}$ is the bhp (bar) at producer i in time period $k \in \mathcal{N}$.

3.3. Single-Shooting Optimization

We use a single shooting algorithm for solution of (7) (Capolei et al., 2012b; Schlegel et al., 2005). Alternatives are multiple-shooting (Bock and Plitt, 1984; Capolei and Jørgensen, 2012) and collocation methods (Biegler, 1984, 2013). Despite the fact that the multiple shooting and the collocation methods offer better convergence properties than the single-shooting method (Biegler, 1984; Bock and Plitt, 1984; Capolei and Jørgensen, 2012), their application in production optimization is restricted by the large state dimension of such problems. The use of multiple-shooting is prevented by the need for computation of state sensitivities. Application of the collocation method is challenging due to the state vector's high dimension and requires advances in iterative methods for solution of large-scale KKT systems to be computationally attractive. Heirung et al. (2011) apply the collocation method for production optimization of a small-scale reservoir.

In the single shooting optimization algorithm, we define the function

$$\begin{aligned} \psi(\{u_k\}_{k=0}^{N-1}, x_0, \theta) = \\ \left\{ \begin{aligned} J &= \int_{t_a}^{t_b} \Phi(x(t), u(t)) dt : \\ x(t_0) &= x_0, \\ \frac{d}{dt} g(x(t)) &= f(x(t), u(t), \theta), t_a \leq t \leq t_b, \\ u(t) &= u_k, t_k \leq t < t_{k+1}, k = 0, 1, \dots, N-1 \end{aligned} \right\} \end{aligned} \quad (11)$$

such that (7) can be expressed as the optimization problem

$$\max_{\{u_k\}_{k=0}^{N-1}} \psi = \psi(\{u_k\}_{k=0}^{N-1}; \bar{x}_0, \theta) \quad (12a)$$

$$s.t. \quad c(\{u_k\}_{k=0}^{N-1}) \leq 0 \quad (12b)$$

Gradient based optimization algorithms for solution of (12) require evaluation of $\psi = \psi(\{u_k\}_{k=0}^{N-1}; \bar{x}_0, \theta)$, $\nabla_{u_k} \psi$ for $k \in \mathcal{N}$, $c(\{u_k\}_{k=0}^{N-1})$, and $\nabla_{u_k} c(\{u_k\}_{k=0}^{N-1})$ for $k \in \mathcal{N}$. For the cases studied in this paper, the constraint function defines linear bounds. Consequently, the evaluation of these constraint functions and their gradients is trivial. Given an iterate, $\{u_k\}_{k=0}^{N-1}$, ψ is computed by solving (7c) marching forwards. $\nabla_{u_k} \psi$ for $k \in \mathcal{N}$ is computed by the adjoint method (Capolei et al., 2012a,b; Jansen, 2011; Jørgensen, 2007; Sarma et al., 2005a; Suwartadi et al., 2012; Völcker et al., 2011).

To solve (12), we use Matlab's `fmincon` function (MATLAB, 2011). `fmincon` provides an interior point and an active-set solver. We use the interior point method since we experienced the lowest computation times with this method. An optimal solution is reported if the KKT conditions are satisfied to within a relative and absolute tolerance of 10^{-6} . The current best but non-optimal iterate is returned in cases when the optimization algorithm uses more than 200 iterations, the relative change in the objective function is less than 10^{-8} , or the relative change in the step size is less than 10^{-8} . Furthermore, the cost function is normalized to improve convergence. We use 4 different initial guesses when running the optimizations. These initial guesses are constant bhp trajectories with the bhp close to the maximal bhp for the injectors and the bhp close to the minimal bhp for the producers. About half of the simulations ended because they exceeded the maximum number of iterations but without satisfying the KKT conditions at the specified tolerance level. In these cases, the relative changes in the cost function and step size were of the order of 10^{-6} . Even if these solutions do not reach our specified tolerances for the KKT conditions, the solutions are sufficiently close to optimality to demonstrate qualitatively the behavior of the mean-variance (MV) optimization. This closeness to optimality is assessed by re-simulation of some of these scenarios with a tolerance limit of 10^{-8} . In these cases, the optimizer converged to a KKT point in about 300 iterations; and we did not observe important differences in these control trajectories compared to the already computed control trajectories.

3.4. Control Constraints

The bhps are constrained by well and reservoir conditions. To maintain the two phase situation, we require the pressure to be above the bubble point pressure (290 bar). To avoid fracturing the rock, the pressure must be below the fracture pressure of the rock (350 bar). To maintain flow from the injectors to the producers, the injection pressure is maintained above 310 bar and the producer pressures are kept below 310 bar. With these bounds, we did not experience that the flow was reversed. Without these pressure bounds, state constraints must be included to avoid flow reversion.

3.5. Certainty Equivalence, Robust, and Mean-Variance Optimization

In reservoir models, geological uncertainty is generally profound because of the noisy and sparse nature of seismic data, core samples, and borehole logs. The consequence of a large number of uncertain model parameters (θ) is the broad range of possible models that may satisfy the seismic and core-sample data. Obviously, the optimal controls, $\{u_k\}_{k=0}^{N-1} = \{u_k(x_0, \theta)\}_{k=0}^{N-1}$, computed as the solution of the finite dimensional optimization problem (12) with the objective function (11) depend on the values of the uncertain parameters, θ . In practice, the initial states, x_0 , will also be uncertain, but in this paper we assume that all uncertainty is contained within θ . When θ is deterministic, the objective function $\psi = \psi(\{u_k\}_{k=0}^{N-1}; x_0, \theta)$ is deterministic and the optimization problem (12) is well defined in the sense that the objective function is a scalar variable. In contrast, when θ is stochastic, $\psi = \psi(\{u_k\}_{k=0}^{N-1}; x_0, \theta)$ is stochastic and the optimization problem (12) is not well defined as ψ is a distribution and not a scalar variable. To define the optimization problem (12) for the stochastic case, a deterministic objective function for (12) must be constructed. The Certainty Equivalence (CE) optimization obtains a deterministic objective function by using the expected value of the uncertain parameters

$$\psi_{CE} = \psi(\{u_k\}_{k=0}^{N-1}; x_0, E_\theta[\theta]) \quad (13)$$

The MV optimization strategy is obtained by using the bi-criterion function

$$\psi_{MV} = \lambda E_\theta[\psi] - (1 - \lambda)V_\theta[\psi] \quad \lambda \in [0, 1] \quad (14)$$

as the objective function in (12). $E_\theta[\psi]$ is the expected value of ψ , and $V_\theta[\psi]$ is the variance of ψ . The term $E_\theta[\psi]$ is related to maximizing return while the term $V_\theta[\psi]$ is related to minimizing risk.

Van Essen et al. (2009) introduce Robust Optimization (RO) for production optimization to reduce the effect of geological uncertainties compared to the CE optimization. The RO objective is

$$\psi_{RO} = E_\theta[\psi] \quad (15)$$

The RO objective, ψ_{RO} , is a special case of the MV objective, ψ_{MV} , i.e. $\psi_{RO} = \psi_{MV}$ for $\lambda = 1$.

We use a Monte Carlo approach for computation of the expected value of parameters, $E_\theta[\theta]$. The expected value of the

return, $E_\theta[\psi]$, and the variance of the return, $V_\theta[\psi]$, are also computed by the Monte Carlo approach. A sample is a set of realizations of the stochastic variables, θ :

$$\Theta_d = \{\theta^1, \theta^2, \dots, \theta^{n_d}\} = \{\theta^i\}_{i=1}^{n_d} \quad (16)$$

This sample is also called an ensemble and is generated by the Monte Carlo method. The objective function values, ψ^i , corresponding to this ensemble are

$$\psi^i = \psi(\{u_k\}_{k=0}^{N-1}; x_0, \theta^i) \quad i = 1, \dots, n_d \quad (17)$$

The sample estimators of the means and the variance are

$$\hat{\theta} = \frac{1}{n_d} \sum_{i=1}^{n_d} \theta^i \quad (18a)$$

$$\hat{\psi} = \frac{1}{n_d} \sum_{i=1}^{n_d} \psi^i \quad (18b)$$

$$\sigma^2 = \frac{1}{n_d - 1} \sum_{i=1}^{n_d} (\psi^i - \hat{\psi})^2 \quad (18c)$$

$\hat{\theta}$ is an estimator for $E_\theta[\theta]$ and $\hat{\psi}$ is an estimator for $E_\theta[\psi]$. σ^2 is an unbiased estimate of $V_\theta[\psi]$. Therefore, σ is an unbiased estimator of the standard deviation $\sigma_\theta[\psi] = \sqrt{V_\theta[\psi]}$.

The CE objective function, ψ_{CE} , is computed using the sample estimator $\hat{\theta} \approx E_\theta[\theta]$, i.e.

$$\psi_{CE} = \psi(\{u_k\}_{k=0}^{N-1}; x_0, \hat{\theta}) \quad (19)$$

Similarly, the MV objective function, ψ_{MV} , is computed using the sample estimators $\hat{\psi} \approx E_\theta[\psi]$ and $\sigma^2 \approx V_\theta[\psi]$, i.e.

$$\psi_{MV} = \lambda \hat{\psi} - (1 - \lambda)\sigma^2 \quad \lambda \in [0, 1] \quad (20)$$

ψ_{MV} is computed by computation of ψ^i for each parameter, $i = 1, \dots, n_d$, and subsequent computation of the sample estimators, $\hat{\psi}$ and σ^2 . The gradient based optimizer used in this paper needs the objective, ψ_{MV} , and the gradients, $\nabla_{u_k} \psi_{MV}$ for $k \in \mathcal{N}$. Appendix A provides an explicit derivation of these gradients. The computation of the objectives and the gradients, ψ^i and $\left\{ \nabla_{u_k} \psi^i \right\}_{k=0}^{N-1}$, can be conducted in parallel for $i = 1, 2, \dots, n_d$. The RO objective based on the sample estimator, $\hat{\psi} \approx E_\theta[\psi]$, is

$$\psi_{RO} = \hat{\psi} \quad (21)$$

The computational effort in computing ψ_{MV} is similar to the computational effort in computing ψ_{RO} . Therefore, no computational penalty is adopted by using the MV approach rather than the RO approach. The CE optimization needs one function and gradient evaluation in each iteration, while the MV optimization needs n_d function and gradient evaluations in each iteration. However, these n_d function and gradient evaluations can be conducted in parallel.

4. Key Performance Indicators

In this section, we present the key performance indicators (KPIs) used to evaluate the optimal control strategies. The KPIs are divided into economic KPIs and production related KPIs. All KPIs related to the mean-variance optimization are functions of the mean-variance trade-off parameter, λ .

4.1. Profit, Risk and Market Solution

Given a control sequence, $\{u_k\}_{k=0}^{N-1}$, computed by some strategy, the NPV may be computed for each realization of the ensemble, $\psi^i = \psi(\{u_k\}_{k=0}^{N-1}; x_0, \theta^i)$ for $i = 1, \dots, n_d$. This gives a set of NPVs, $\{\psi^i\}_{i=1}^{n_d}$. By itself, these NPVs and their distribution are of interest. Economic KPIs such as NPV mean, NPV standard deviation, ratio of NPV mean to NPV standard deviation, and the minimum and maximum NPV in the finite set are used to summarize and evaluate the performance of a given control strategy, $\{u_k\}_{k=0}^{N-1}$. Given $\{\psi^i\}_{i=1}^{n_d}$, the expected mean NPV may be approximated using (18b), $E_\theta[\psi] \approx \hat{\psi}$. Similarly, the standard deviation of the mean may be approximated using (18c), $\sigma_\theta[\psi] \approx \sigma$. The ratio of return and risk is called the Sharpe ratio and is defined as (Sharpe, 1994)

$$S_h = \frac{E_\theta[\psi]}{\sigma_\theta[\psi]} \approx \frac{\hat{\psi}}{\sigma} \quad (22)$$

The ensemble, $\{\psi^i\}_{i=1}^{n_d}$, is finite. Therefore, the minimum and maximum NPV may be computed by

$$\psi_{\min} = \min \{\psi^i\}_{i=1}^{n_d} \quad (23a)$$

$$\psi_{\max} = \max \{\psi^i\}_{i=1}^{n_d} \quad (23b)$$

Given an optimal control sequence, $\{u_k\}_{k=0}^{N-1}$, ψ_{\min} is the lowest NPV in the ensemble of permeability fields and ψ_{\max} is the highest NPV in the ensemble of permeability fields.

The economic KPIs, $\{\hat{\psi}, \sigma, S_h, \psi_{\min}, \psi_{\max}\}$, provide a set of values that may be used to quickly evaluate and compare different control strategies, $\{u_k\}_{k=0}^{N-1}$, in terms of return and risk. Subsequently, selected solutions, $\{u_k\}_{k=0}^{N-1}$, may be evaluated in detail by inspection of the distribution of $\{\psi^i\}_{i=1}^{n_d}$ and by inspection of the solution trajectories, $\{u_k\}_{k=0}^{N-1}$. The idea in the mean-variance model is to compute the optimal solution for different values of the return-risk trade-off parameter, $\lambda \in [0, 1]$, and select the parameter λ to obtain the best trade-off between return and risk (Markowitz, 1952; Steinbach, 2001). As part of the mean-variance optimization, the NPV of each realization of the ensemble is computed for various values of λ in the mean-variance objective function (20). This gives $\{\psi^i(\lambda)\}_{i=1}^{n_d}$ and $\{u_k(\lambda)\}_{k=0}^{N-1}$ for a range of values of the mean-variance trade-off parameter, $\lambda \in [0, 1]$. For each value of λ , the set of ensemble NPVs and (18b) are used to approximate the expected NPV as function of λ , $E_\theta[\psi(\lambda)] \approx \hat{\psi}(\lambda)$. Similarly, the set of ensemble NPVs and (18c) are used to approximate the standard deviation of the NPV as function of λ , $\sigma_\theta[\psi(\lambda)] \approx \sigma(\lambda)$. The expected NPV, $E_\theta[\psi(\lambda)]$, and the risk $\sigma_\theta[\psi(\lambda)]$, may be plotted and tabulated as a function of λ . This gives some overview of the behaviour of key economic performance indicators such as

expected profit and risk as a function of λ . Also a phase plot of risk versus return, $\{\sigma_\theta[\psi(\lambda)], E_\theta[\psi(\lambda)]\}$ for $\lambda \in [0, 1]$, illustrates the risk-return relationship of the mean-variance model. The efficient frontier is the curve that yields the maximal return as function of risk. By itself, the efficient frontier does not provide a unique solution to the production optimization problem. The efficient frontier provides only efficient pairs of return and risk; the preferred solution depends on the risk preferences of the decision maker. One way to choose a solution among the efficient risk-return pairs is to choose the solution that maximizes the Sharpe ratio (22) (Sharpe, 1994). The solution that maximizes the Sharpe ratio is called the market solution.

4.2. Cumulative Productions Indicators

In addition to the economic KPIs, we also consider production related KPIs. The production related KPIs are the expected cumulative oil production, the expected cumulative water injection, and the production efficiency.

The cumulative oil production, $Q_o(t)$, and the cumulative water injection, $Q_{w,inj}(t)$, at time t are given by

$$Q_o(t) = \int_0^t \left(\sum_{i \in \mathcal{P}} q_{o,i} \right) dt \quad (24a)$$

$$Q_{w,inj}(t) = \int_0^t \left(\sum_{i \in \mathcal{I}} q_i \right) dt \quad (24b)$$

We approximate the cumulative oil production (24a) and water injection (24b) at final time t_b by using the right rectangle (implicit Euler) integration method

$$Q_o = Q_o(t_b) = \sum_{k=0}^{N-1} \left(\sum_{i \in \mathcal{P}} q_{o,i}(x_{k+1}, u_k) \right) \Delta t_k \quad (25a)$$

$$Q_{w,inj} = Q_{w,inj}(t_b) = \sum_{k=0}^{N-1} \left(\sum_{i \in \mathcal{I}} q_i(x_{k+1}, u_k) \right) \Delta t_k \quad (25b)$$

and we compute the expected values of the cumulative productions (25a)-(25b) as the sample averages

$$E_\theta[Q_o] = \frac{1}{n_d} \sum_{i=1}^{n_d} Q_o^i \quad (26a)$$

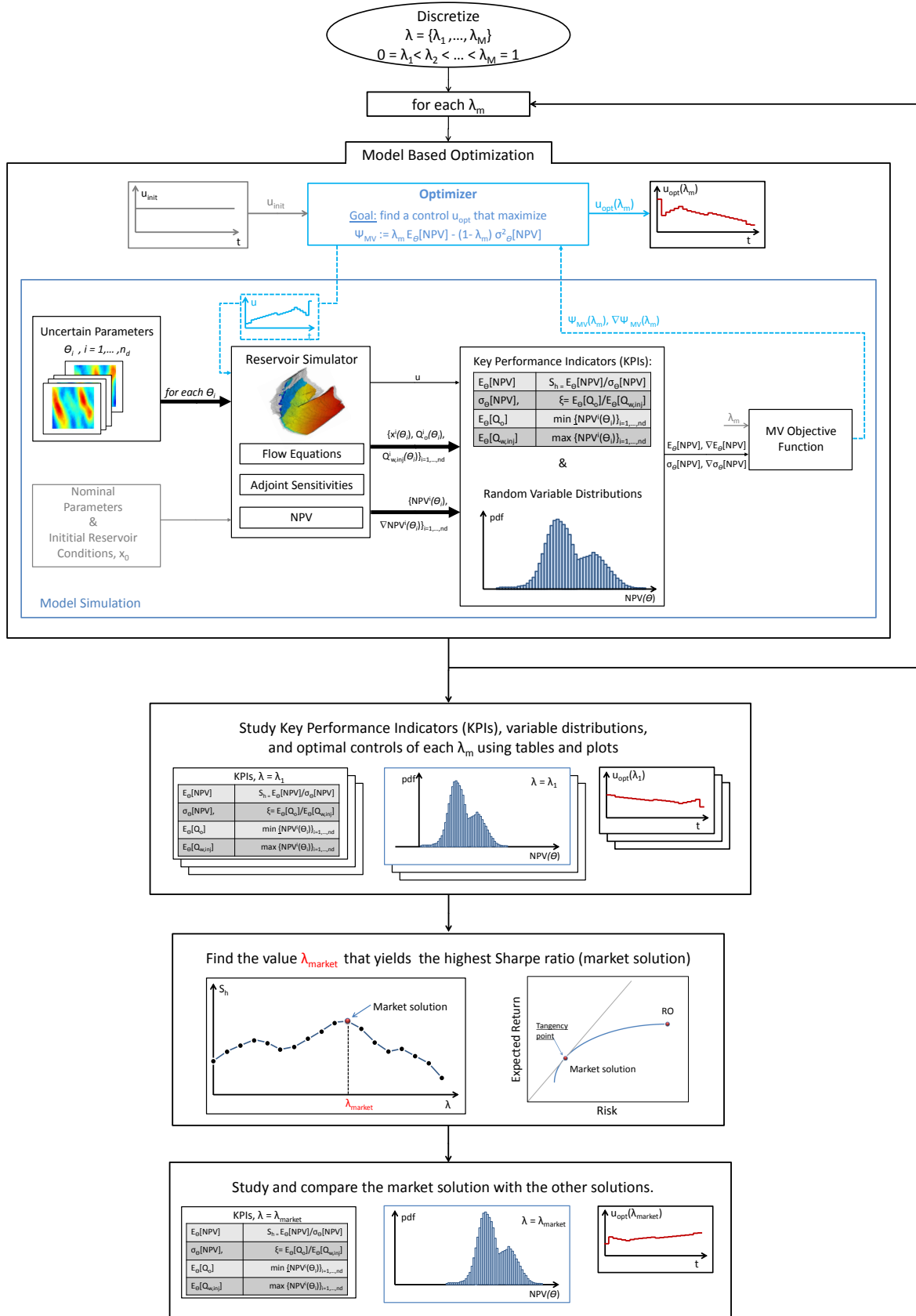
$$E_\theta[Q_{w,inj}] = \frac{1}{n_d} \sum_{i=1}^{n_d} Q_{w,inj}^i \quad (26b)$$

Superscript i refers to the quantity computed using realization i . The production efficiency, ξ , is defined and computed as the volumetric ratio of the produced oil and the injected water

$$\xi = \frac{E_\theta[Q_o]}{E_\theta[Q_{w,inj}]} \quad (27)$$

4.3. Mean-Variance Optimization and the Market Solution

The flowchart in Fig. 2 summarizes the mean-variance based optimization procedure to obtain the market solution. First, the mean-variance trade-off parameter, $\lambda \in [0, 1]$, is discretized into



KPIs, $\lambda = \lambda_1$	
$E_{\theta}[NPV]$	$S_h = E_{\theta}[NPV]/\sigma_{\theta}[NPV]$
$\sigma_{\theta}[NPV]$	$\xi = E_{\theta}[Q_c]/E_{\theta}[Q_{w,ini}]$
$E_{\theta}[Q_c]$	$\min \{NPV(\theta)\}_{i=1, \dots, nd}$
$E_{\theta}[Q_{w,ini}]$	$\max \{NPV(\theta)\}_{i=1, \dots, nd}$

$\lambda = \lambda_1$

KPIs, $\lambda = \lambda_{market}$	
$E_{\theta}[NPV]$	$S_h = E_{\theta}[NPV]/\sigma_{\theta}[NPV]$
$\sigma_{\theta}[NPV]$	$\xi = E_{\theta}[Q_c]/E_{\theta}[Q_{w,ini}]$
$E_{\theta}[Q_c]$	$\min \{NPV(\theta)\}_{i=1, \dots, nd}$
$E_{\theta}[Q_{w,ini}]$	$\max \{NPV(\theta)\}_{i=1, \dots, nd}$

$\lambda = \lambda_{market}$

Figure 2: Flowchart of the model based optimization procedure using the mean-variance objective to obtain the market solution.

a finite number of values $\{\lambda_m\}_{m=1}^M$. For each of these values ($\lambda_m, m = 1, 2, \dots, M$), we do model based optimization based on the mean-variance objective function. The results from the model based optimization are a function of λ_m . For each value of the mean-variance parameter, $\{\lambda_m\}_{m=1}^M$, the results from the model based optimization are the optimal bottom-hole pressures, $u_{\text{opt}}(\lambda_m)$, the NPV distribution, and the KPIs. The market solution is determined by selecting the value of the mean-variance trade-off parameter, λ_{market} , that maximizes the Sharpe ratio. We select and implement the bottom-hole pressures corresponding to the market solution and get the NPV distribution as well as the KPIs corresponding to the market solution.

5. Simulated Test Cases

The mean-variance optimization strategy is studied for two test cases. We discretize λ by choosing 16 points in the interval $[0, 1]$. The first 5 points are equidistantly spaced (in the λ -space), while the remaining points are selected manually and adaptively by inspection of the efficient frontier such that the points in the efficient frontier are approximately equidistantly spaced. The same reservoir permeability fields and petro-physical parameters are used for the two test cases. Fig. 3 illustrates the ensemble of permeability fields used to represent the uncertain reservoir. Fig. 4 illustrates the mean permeability field of the ensemble of permeability fields. As illustrated by Fig. 5 and reported in Table 1, the difference between the two test cases are the well configurations and the economical parameters. Test Case I contains more injector wells than Test Case II. Furthermore, the water injection costs and the water separation costs are higher in Test Case I than in Test Case II. This implies that a reactive strategy that injects water at a maximal rate is penalized in Test Case I due to the high water injection and water separation costs. Test Case I is used to illustrate a complicated well configuration benefitting from intelligent coordination of wells and penalizing conventional reactive strategies. Test Case II is simpler and the value of feedback becomes more important than predictive coordination of the wells. This means that in Test Case II a feedback based reactive strategy will be able to do better than a model based open loop strategy. Combined, the two test cases illustrates that the shape and geometry of the efficient frontier is case dependent, that the value of feedback in a reactive strategy compared to an open-loop optimization strategy is dependent on the well configuration, and that the mean-variance objective formulation is an efficient way to trade off risk and return.

5.1. Uncertain Parameters

In our study, the permeability field is the uncertain parameters. We generate 100 permeability field realizations of a 2D reservoir in a fluvial depositional environment with a known vertical main-flow direction. Fig. 3 illustrates such an ensemble of permeability fields. These permeability realizations are equal to the permeabilities used by Capolei et al. (2013). To generate the permeability fields, we first create a set of 100 binary (black and white) training images by using the sequential

Table 1: Petro-physical and economical parameters for the two phase model and the discounted state cost function used in the case studies. TC I = Test Case I. TC II = Test Case II.

	Description	Value	Unit
ϕ	Porosity	0.2	-
c_r	Rock compressibility	0	Pa ⁻¹
ρ_o	Oil density (300 bar)	700	kg/m ³
ρ_w	Water density (300 bar)	1000	kg/m ³
μ_o	Dynamic oil viscosity	$3 \cdot 10^{-3}$	Pa · s
μ_w	Dynamic water viscosity	$0.3 \cdot 10^{-3}$	Pa · s
S_{or}	Residual oil saturation	0.1	-
S_{ow}	Connate water saturation	0.1	-
n_o	Corey exponent for oil	2	-
n_w	Corey exponent for water	2	-
P_{init}	Initial reservoir pressure	300	bar
S_{init}	Initial water saturation	0.1	-
r_o	Oil price	120	USD/bbl
r_{wp}	Water separation cost (TC I)	25	USD/bbl
r_{wp}	Water separation cost (TC II)	20	USD/bbl
r_{wi}	Water injection cost (TC I)	15	USD/bbl
r_{wi}	Water injection cost (TC II)	10	USD/bbl
d	Discount factor	0	-

Monte Carlo algorithm 'SNESIM' (Liu, 2006). Then a Kernel PCA procedure is used to preserve the channel structures and to smooth the original binary images (Schölkopf et al., 1998). The realizations obtained by this procedure are quite heterogeneous. The values of the permeabilities are in the range 6 – 2734 mD.

5.2. Description of the Test Cases

We consider a conventional horizontal oil field that can be modeled as two phase flow in a porous medium (Chen, 2007). The reservoir size is 450 m × 450 m × 10 m. By spatial discretization, this reservoir is divided into 45 × 45 × 1 grid blocks. The permeability field is uncertain, $\theta = \ln K$. We assume that the ensemble in Fig. 3 represents the range of possible geological uncertainties.

Table 1 lists the reservoir's petro-physical and economical parameters. The initial reservoir pressure is 300 bar everywhere in the reservoir. The initial water saturation is 0.1 everywhere in the reservoir. This implies that initially, the reservoir has a uniform oil saturation of 0.9. The manipulated variables are the bhps over the life of the reservoir. In this study, we consider a zero discount factor, d , in the cost function (8). This means that we maximize NPV at the final time without short term production considerations (Capolei et al., 2012b).

In both test cases, we consider a prediction horizon of $t_N = 4 \cdot 365 = 1460$ days divided in $N = 60$ control periods (i.e. the control period is $T_s \approx 24$ days). We control the reservoir using three strategies: a reactive strategy, a CE strategy, and a MV strategy. The RO strategy is considered a special MV strategy with $\lambda = 1$. In the reactive strategy, we develop the field at the maximum production rate by setting the producers

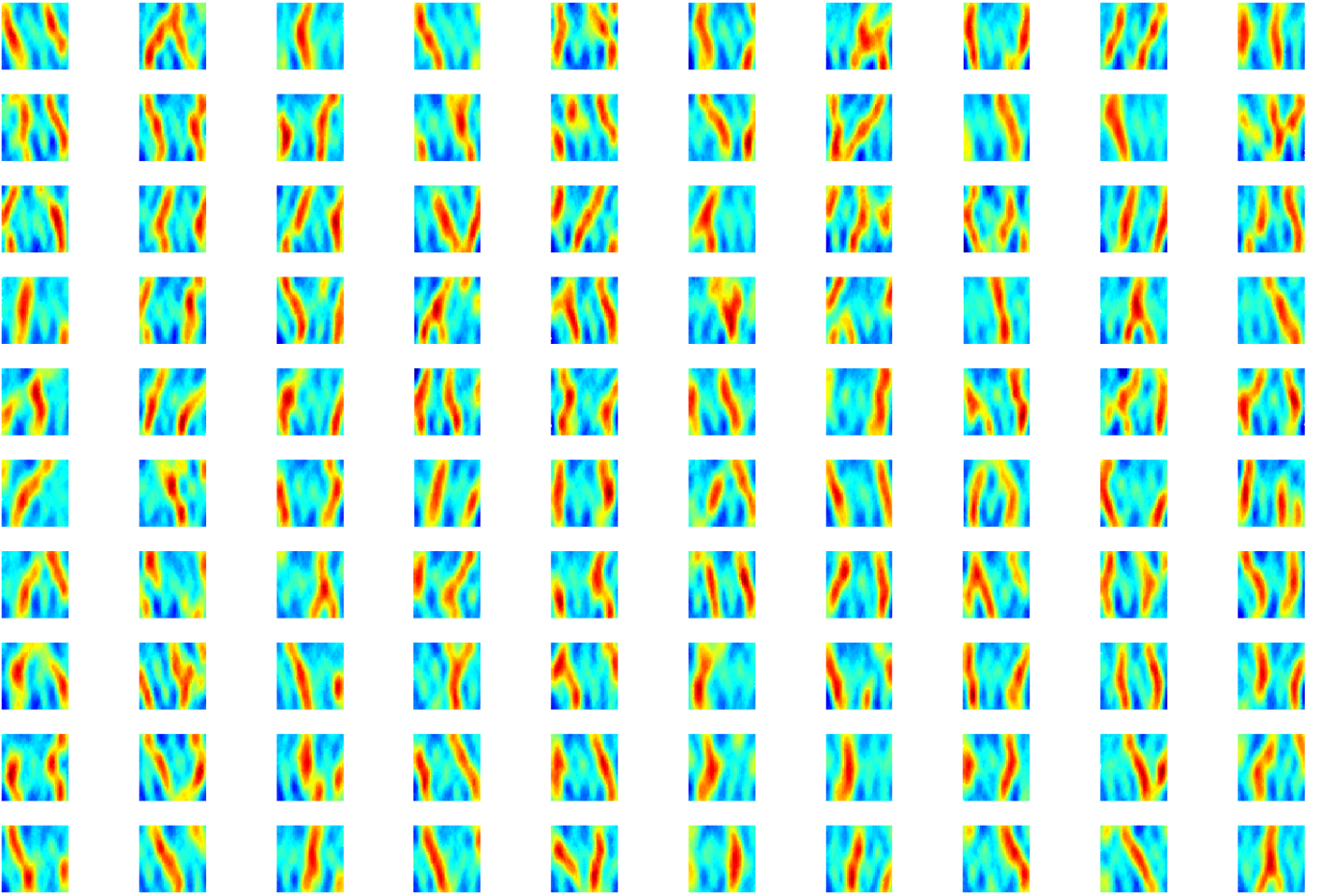


Figure 3: Plots of the permeability fields used to describe the uncertain reservoir. An ensemble of 100 realizations is used. The realizations are quite heterogeneous. The permeability values are in the range 6 – 2734 mD. The logarithm of the permeability is plotted for better visualization.

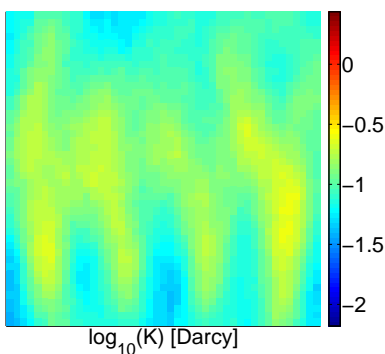


Figure 4: A plot of the mean permeability field for the ensemble of permeability fields in Fig. 3. The mean is a smoothed version of the ensembles. Due to the heterogenous nature of the ensembles, the mean does not necessarily reflect the channel structure of any of the ensemble members.

at the lowest allowed bhp value (290 bar) and the injectors at the maximum allowed bhp value (350 bar). When a production well is no longer economical, it is shut in. A production well is uneconomical when the value of the produced oil is less than the separation cost of the produced water. The CE strategy is based on solving problem (12) using the CE cost function ψ_{CE} (19). It uses the mean (Fig. 4) of the ensemble (Fig. 3) as its permeability field. The MV strategy is based on solving problem (12) using the cost function ψ_{MV} (20) for different values of the parameter λ .

5.3. Test Case I

Fig. 5a illustrates the well configuration for Test Case I. Test Case I has 9 injection wells and 4 producer wells. Table 1 contains the petro-physical as well as the economic parameters. From the oil price and the water separation cost for Test Case I, it is apparent that a producer well becomes uneconomical when the fractional flow, f_w , exceeds $r_o/(r_o + r_{wp}) = 120/(120 + 25) = 0.828$.

Fig. 6 shows the optimal bhp trajectories for the producer wells while Fig. 7 shows the optimal bhp trajectories for the in-

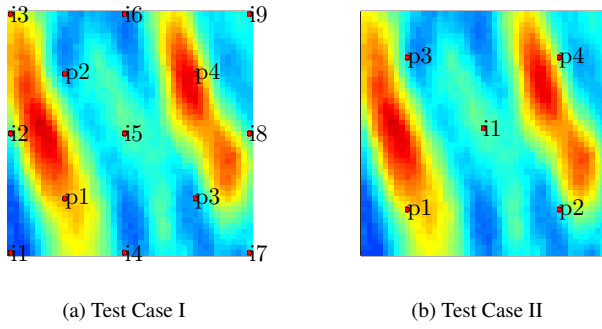


Figure 5: The well configuration for Test Case I and II. The permeability field in this plot is the permeability field in the upper left corner of Fig. 3. Producer wells are indicated by the letter p, and injector wells are indicated by the letter i. In addition to the injector and producer wells in Test Case II, Test Case I has a number of injector wells at the boundary of the field.

jector wells. These trajectories are computed using the reactive, the MV, the RO, and the CE optimization strategy. $\lambda = 0.59$ gives the market solution for this case, and this value of λ is used in the MV strategy. Compared to the RO and the market MV strategy, the CE trajectories do not contain sudden large changes in the bhp. This is due to the fact that the mean permeability field used by the CE strategy does not have sharp edges. It is also apparent that the bhp trajectories of the RO strategy have larger sudden changes than the trajectories of the market MV strategy. For some realizations of the permeability field, the RO trajectories would perform very well because they utilize the sharp channel structure in the permeability field. However, sudden large changes in the manipulated variables is an indication of solutions that are sensitive to process noise and model uncertainties. As sensitivity to noise is related to high risk, the trajectories of the bore hole pressures indicate that the RO strategy is more risky than the market MV strategy. Fig. 8 confirms this observation.

Fig. 8 illustrates the profit, ψ^i , for each realization of the permeability field using the reactive strategy as well as the CE, the RO, and the market MV optimal control strategies. The average profit over the realizations is a measure of the expected return, while the fluctuations are a measure of risk. For each control strategy, the bigger the fluctuations in profit, the bigger the related risk. It is evident that the CE strategy has the lowest expected return and the biggest risk. The CE strategy also has the lowest worst case return. The reactive strategy has a mean return that is higher than the mean return of the CE strategy but lower than the mean returns of the RO and the MV strategies. The risk for the reactive strategy is lower than the risk for the CE strategy but higher than the risks for the RO and the MV strategies. Comparing the market MV and the RO strategies, the RO strategy has a slightly higher mean profit than the market MV strategy but at the price of a significantly higher risk.

Table 2 reports KPIs for each control strategy. The econom-

ical KPIs are the expected NPV, the standard deviation NPV, the Sharpe ratio, and the minimum and maximum NPV for the ensemble. The production related KPIs are the mean oil production, the mean water injection, and the production efficiency (27) for the ensemble. The mean oil production and the mean water injection are scaled by the pore volume of the reservoir. Interestingly, the MV market strategy ($\lambda = 0.59$) has the highest minimum ensemble NPV value, ψ_{\min} . This means that in this case, the market solution has a better worst case profit, ψ_{\min} , compared to all other control strategies including the MV strategies with lower standard deviation. Compared to the CE strategy and the reactive strategy, all MV control trajectories give higher expected NPV and lower NPV standard deviation. In that sense, the MV solutions are said to dominate the CE solution and the solution given by the reactive strategy. The RO solution has the highest maximum NPV and also the highest expected NPV. However, among the MV solutions, it is also the solution with the lowest minimum NPV. This implies that the RO solution is very risky and this is confirmed by its high NPV standard deviation. Among the MV solutions, the RO solution has the highest NPV standard deviation. Fig. 9 summarizes the economic KPIs of the MV solutions. Fig. 9a shows the expected NPV as well as the worst and best NPV for the ensemble as function of the mean-variance trade-off parameter, λ . It is easily observed that the market MV solution, coincidentally, is also the max-min solution, i.e. the solution yielding the highest worst case NPV. Similarly, the high risk of the RO solution is evident. Fig. 9b illustrates the standard deviation of the NPV as function of the mean-variance trade-off parameter, λ . The standard deviation of the NPV is a measure of risk. The risk is a non-monotonous function of the mean-variance trade-off parameter, λ . Measured by NPV standard deviation, the minimum risk solution is obtained for $\lambda = 0.125$. However, this solution is inferior to the market MV solution, as the market MV solution has a higher worst case NPV, a higher mean NPV, and a higher best case NPV (see Fig. 9a). Fig. 9c plots the Sharpe ratio as function of the mean-variance trade-off parameter, λ . This plot indicates that the maximal Sharpe ratio, i.e. the market solution, is obtained for $\lambda = 0.59$. The Sharpe ratio is not a concave function of λ in this case. Another local maximum with almost the same Sharpe ratio as the global maximum is obtained for $\lambda = 0.125$, i.e. for the minimum risk solution. As we noted previously, this solution is inferior to the market solution. Also note that the RO solution has the lowest Sharpe ratio. Fig. 9d illustrates the risk-return relations for the different MV strategies as well as the CE, the RO (MV with $\lambda = 1$), and the reactive strategy. This figure clearly illustrates the superiority of the market MV strategy over the reactive strategy and the CE strategy. It also shows the reduced risk of the market MV strategy compared to the RO strategy at the cost of slightly reduced mean profit. The risk-return curve for the MV optimization strategies has two arcs. The efficient frontier arc is the blue curve in Fig. 9d; the red curve is the inefficient frontier. In the efficient frontier, an increased risk is associated with an increased mean return. The MV strategy contains some risk-return points that are feasible but not on the efficient frontier, i.e. points that for a given risk level do not produce the

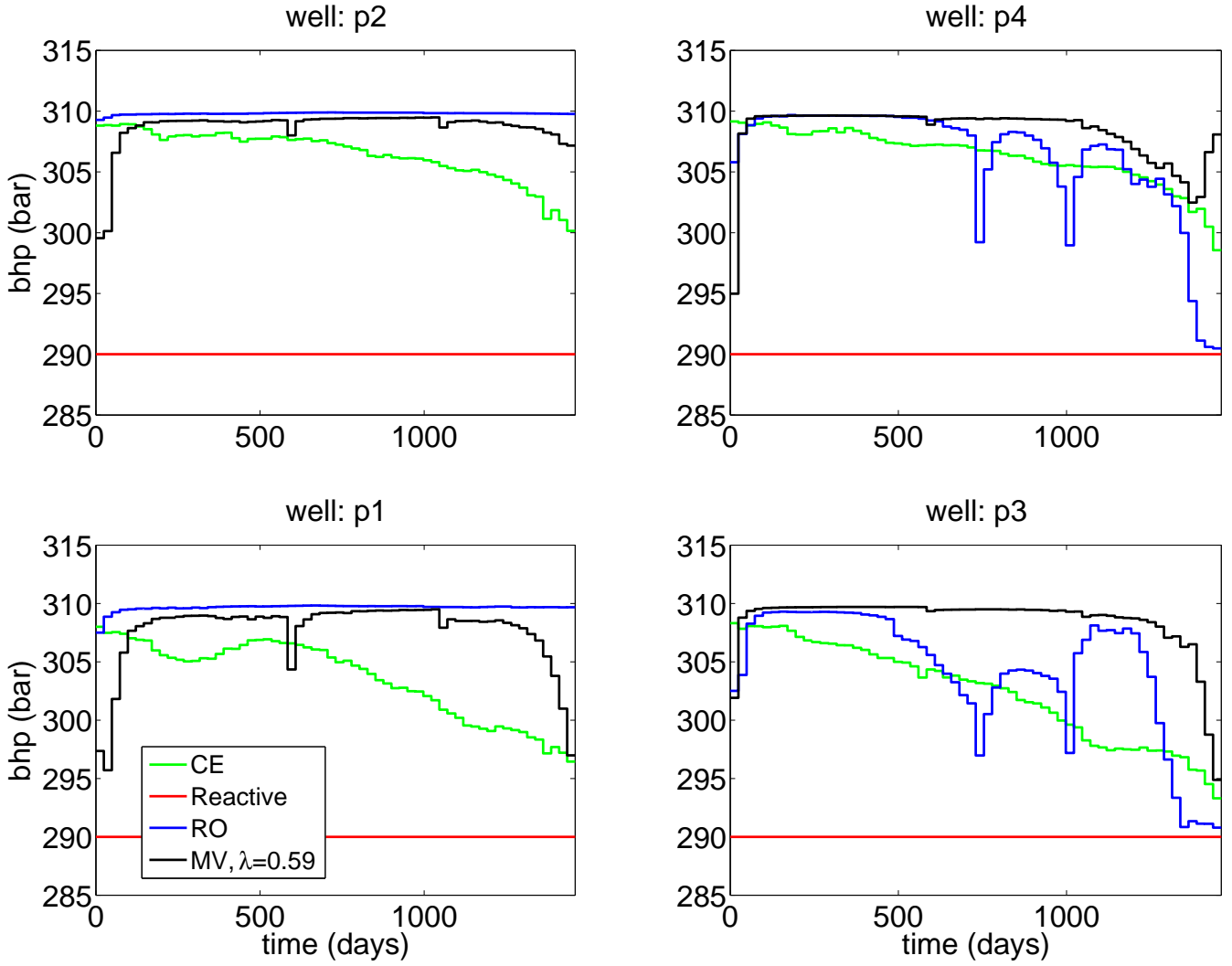


Figure 6: Test Case I. Trajectories of the bhp at producer wells using different optimization strategies. In the reactive strategy, the producer wells are shut in when production becomes uneconomical. The shut in time is different for each realization and is not indicated in the plot.

Table 2: Key Performance Indicators (KPIs) for Test Case I. The economic KPIs are the expected profit, the standard deviation of the profit, the Sharpe ratio, and the minimum and maximum profit for the ensemble. The reported production related KPIs are the expected oil production, the expected water injection, and the production efficiency, ξ . The productions are normalized by the pore volume. All improvements are relative to the reactive strategy.

Strategy	$\hat{\psi}$		σ		S_h	ψ_{\min}		ψ_{\max}		$E_{\theta}[Q_o]$		$E_{\theta}[Q_{w,inj}]$		ξ
	10 ⁶ USD, %		10 ⁶ USD, %			10 ⁶ USD, %		10 ⁶ USD, %		%		%		
Reactive	39.04,	/	9.01,	/	4.34	17.62,	/	60.47,	/	0.39,	/	1.04,	/	37.8
CE	28.57,	-26.8	18.93,	+110.2	1.51	-23.86,	-235.4	60.25,	-0.40	0.32,	-18.4	0.88,	-15.3	36.4
MV														
$\lambda = 1$ (RO)	50.40,	+29.1	8.17,	-9.3	6.17	28.11,	+67.2	69.90,	+15.6	0.26,	-34.0	0.44,	-57.4	58.5
$\lambda = 0.75$	48.00,	+25.0	6.13,	-32.0	7.83	34.68,	+96.8	64.52,	+6.7	0.24,	-38.9	0.39,	-62.5	61.6
$\lambda = 0.59$	47.09,	+20.6	4.89,	-45.7	9.63	35.44,	+101	57.747,	-4.5	0.23,	-40.9	0.38,	-63.6	61.5
$\lambda = 0.5$	45.58,	+16.7	5.15,	-42.8	8.85	33.13,	+88.0	57.84,	-4.3	0.23,	-41.0	0.39,	-62.4	59.3
$\lambda = 0.25$	45.09,	+15.5	4.76,	-47.1	9.47	32.39,	+83.8	56.3,	-6.9	0.22,	-42.5	0.37,	-64.0	60.3
$\lambda = 0.125$	44.00,	+12.7	4.61,	-48.8	9.54	31.73,	+80.1	54.67,	-9.6	0.22,	-44.1	0.36,	-65.1	60.5
$\lambda = 0$	41.57,	+6.5	5.02,	-44.2	8.28	29.47,	+67.2	52.40,	-13.3	0.21,	-45.6	0.36,	-64.9	58.6

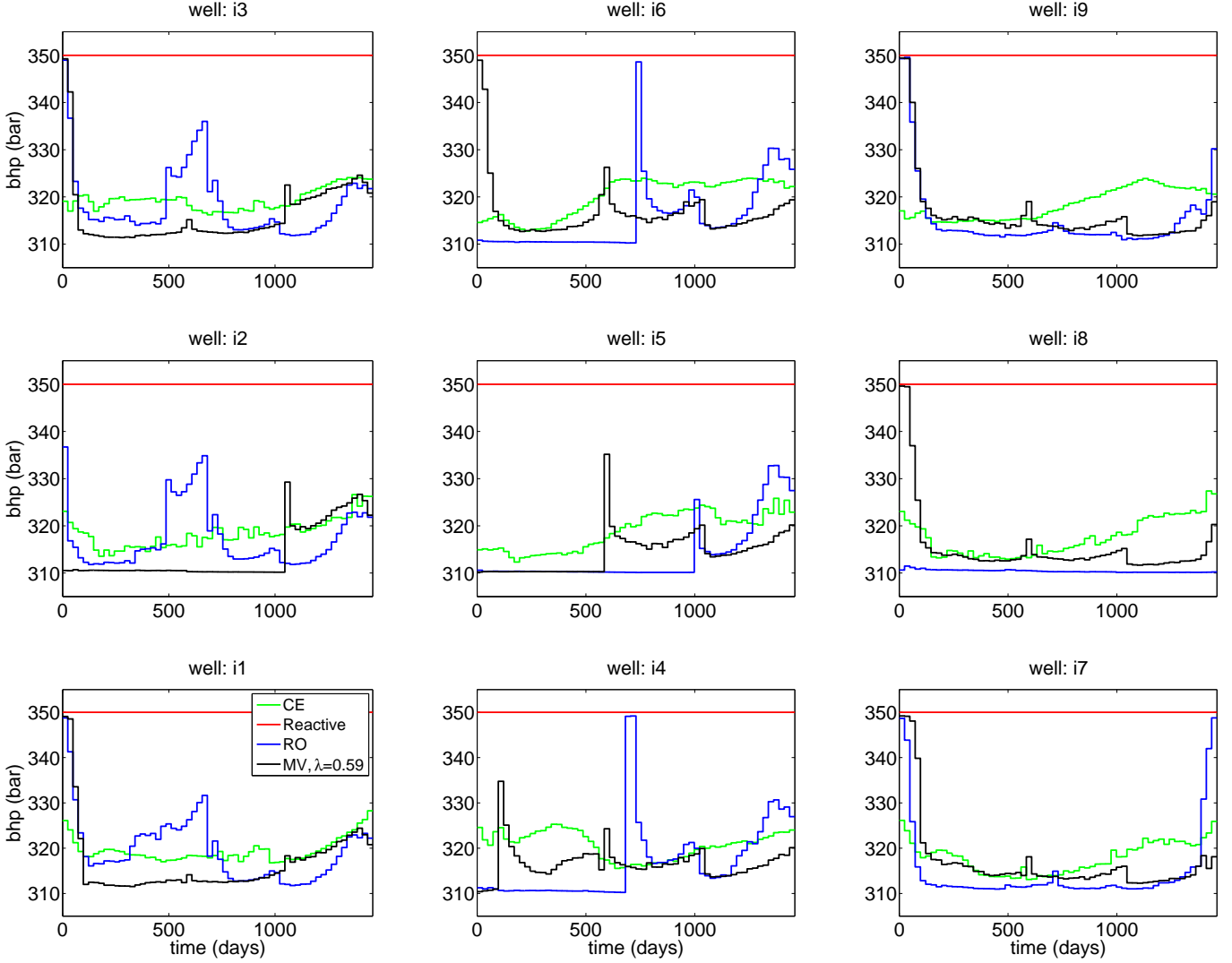


Figure 7: Test Case I. Trajectories of bhp for injector wells using different optimization strategies.

maximal expected return.

For Test Case I, the production related KPIs in Table 2 demonstrate that the reactive strategy produces much more oil compared to the other control strategies. However, it also injects and produces much more water, i.e. $E_\theta[Q_o] = 0.39$ pore volume and $E_\theta[Q_{w,inj}] = 1.04$ pore volume. From a pure production point of view, the most efficient MV solution does not coincide with the market solution nor with the RO solution. It occurs for $\lambda = 0.75$ and has a production efficiency of $\xi = 61.6\%$, i.e. 61.6 barrels of oil is produced for 100 barrels of injected water.

5.4. Test Case II

Fig. 5b indicates the well configuration of Test Case II. Table 1 reports the petro-physical and economical parameters used for the simulations. The economic parameters imply that a producer well becomes non-economical when the fractional water flow, f_w , exceeds $r_o/(r_o + r_{wp}) = 120/(120 + 20) = 0.857$. Com-

pared to Test Case I, Test Case II has fewer injection wells and the water separation cost is lower.

Fig. 10 and Table 3 report the economic KPIs for Test Case II. They summarize and provide an overview of the performance of different control strategies for Test Case II. The Sharpe ratio curve in Fig. 10c indicates that the market MV solution is obtained for $\lambda = 0.125$. As illustrated by the efficient frontier in the risk-return plot in Fig. 10d, the RO solution and the CE solution both have higher expected return as well as significantly higher risk (NPV standard deviation) than the MV market solution. Comparing with the sketch in Fig. 1, the efficient frontier illustrated in Fig. 10d is a textbook example of the relation between risk and return. At the price of a low reduction in the expected return, the MV market solution decreases the risk significantly compared to the RO solution and the CE solution. Also the worst case NPV is much higher for the MV market solution than the corresponding values for the RO solution and the CE solution. The worst case NPV, ψ_{\min} , is even negative for the CE solution.

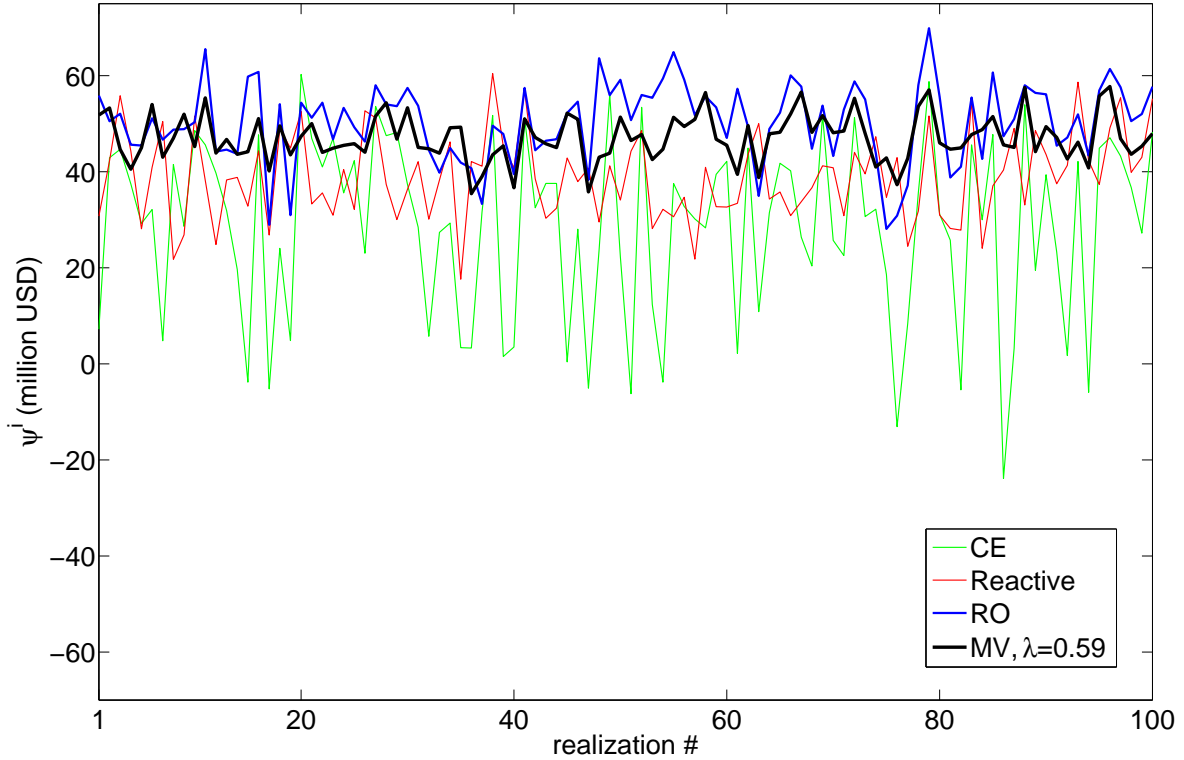


Figure 8: Test Case I. The net present value (NPV) of the optimal solution for each realization of the ensemble. The optimal solution is computed using a CE objective, a RO objective, and a MV objective with a mean-variance trade-off corresponding to the market solution ($\lambda = 0.59$). We also show the NPVs for the reactive strategy.

Test Case II has been included to demonstrate the value of information and feedback. While the optimization based strategies studied in this paper are open-loop strategies that do not use feedback, the reactive strategy is a feedback controller. As reported in Fig. 10d and Table 3, the reactive strategy has both a higher expected NPV and a lower risk (NPV standard deviation) than the RO solution as well as the CE solution. Consequently, the reactive solution is superior to the open-loop CE and RO strategies. Furthermore, the worst case NPV of the reactive strategy is higher than the worst case NPVs of the CE solution and the RO solution. The worst case NPV of the reactive strategy is even better than the mean NPV of the CE strategy. Fig. 10d illustrates that the reactive strategy has a significantly higher return than the MV market solution. However, the reactive strategy also has a higher risk measured by the NPV standard deviation. Nevertheless, the reactive strategy is still superior to the MV market solution as the worst case NPV of the reactive strategy is larger than the best case NPV of the market MV solution. This illustrates that even though a control strategy may have a larger standard deviation than another control strategy, it may still be superior as all its possible profits are larger than the profits of the other control strategy.

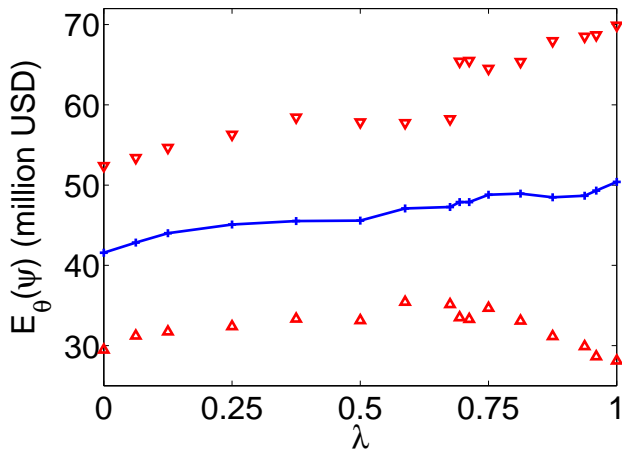
Interestingly and perhaps surprising, Fig. 10a as well as Table 3 indicate that the Market MV solution is in some sense

inferior to the MV solution obtained for $\lambda = 0.25$. The MV solution for $\lambda = 0.25$ has a worst case NPV, a mean NPV, and a best case NPV, that are all higher than the corresponding values for the market solution. Even though the market solution has lower risk in terms of standard deviation of the NPV, this becomes in some sense irrelevant as both the mean NPV and the worst case NPV of the MV solution with $\lambda = 0.25$ are higher than the corresponding values of the market solution. A more detailed comparison of the two MV strategies would require the distribution of the NPVs for the two strategies and not only the just discussed statistics.

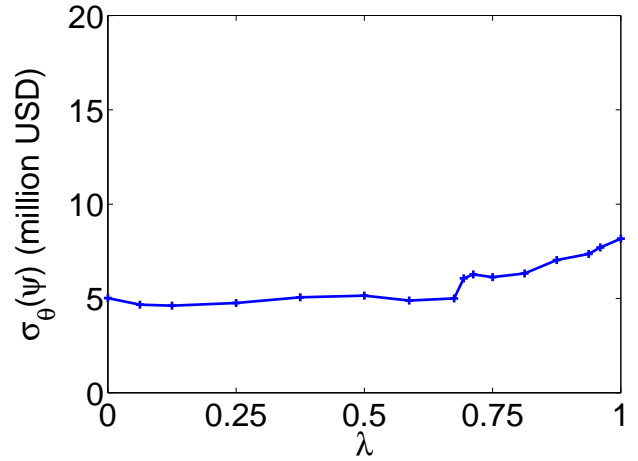
In addition to economic KPIs, Table 3 also reports the production related KPIs. The reactive strategy has the highest oil recovery but also the highest water injection such that its production efficiency, ξ , is the lowest among all strategies. The most efficient solution measured by the production efficiency, ξ , would be the minimum variance solution obtained for $\lambda = 0$. This solution would have a production efficiency of $\xi = 81.9\%$. In economic terms, this solution would still be inferior to the reactive strategy.

5.5. Discussion

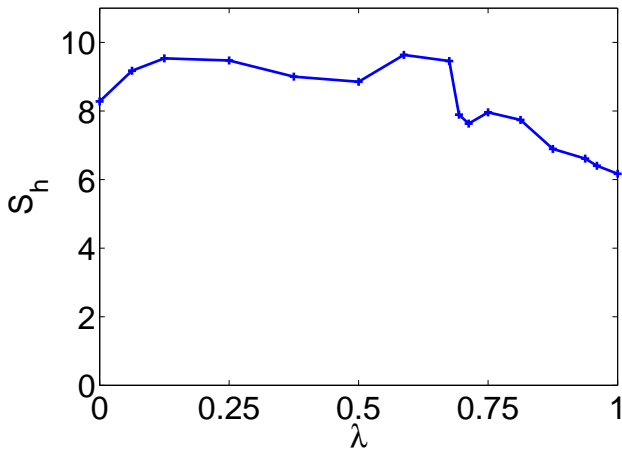
Using two test cases, we demonstrated production optimization of an uncertain oil reservoir by open-loop optimal control



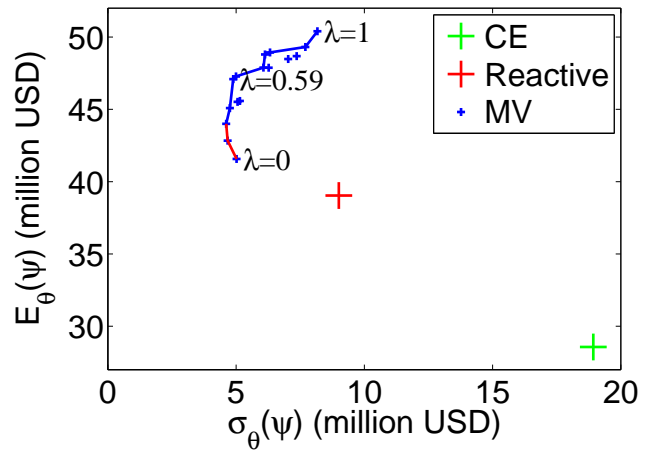
(a) Expected profit, max profit, and min profit.



(b) Risk measured as the standard deviation of profit.



(c) The Sharpe ratio.



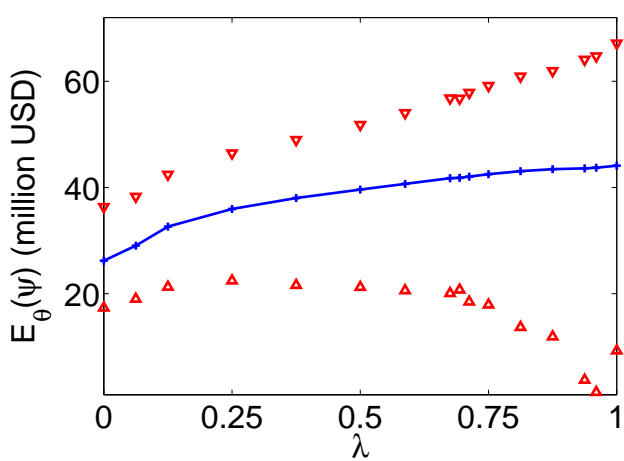
(d) A risk-return plot. The expected NPV vs standard deviation of NPV.

Figure 9: Mean-variance relations for Test Case I. Profit (a), risk (b), and Sharpe Ratio (c) for different mean-variance trade-offs, λ . (d) is a phase plot of expected profit vs risk measured as the standard deviation of profit. The blue curve is the efficient frontier. The red curve is the inefficient frontier. Also the CE solution and the reactive solution are indicated.

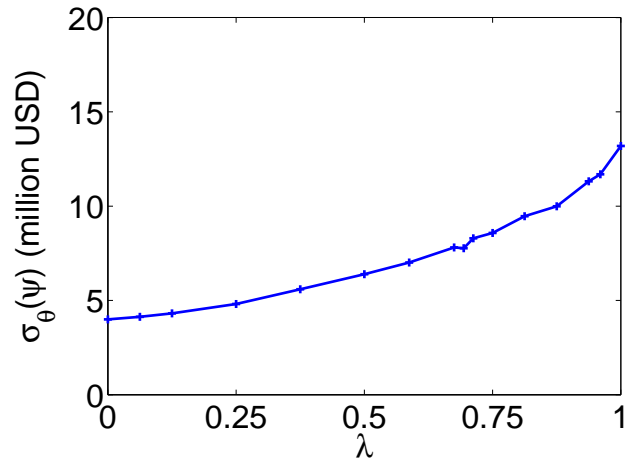
using a mean-variance objective function. We compared optimal control using a mean-variance objective function to open-loop optimal control with a CE objective function and an RO objective function, respectively. For uncertain reservoirs, the market solution of the mean-variance objective provides better and more well-behaved bhp trajectories with less risk (standard deviation) of the NPV. This reduced risk typically comes at the price of reduced profit. The simulations revealed that for the reservoirs in this paper, the reduction in expected NPV is modest compared to the risk reduction. Risk mitigation by the mean-variance objective can be regarded as a regularization of the RO objective and has the same regularizing effect on the solution, i.e. the bhp trajectories, as the effect of e.g. a Tikhonov regularizer in least squares problems (Hansen, 1998).

The analysis, evaluation and discussion of control performance in uncertain oil reservoirs is facilitated by Fig. 9 and Fig. 10. In practice, a dash board of risk-return relations sim-

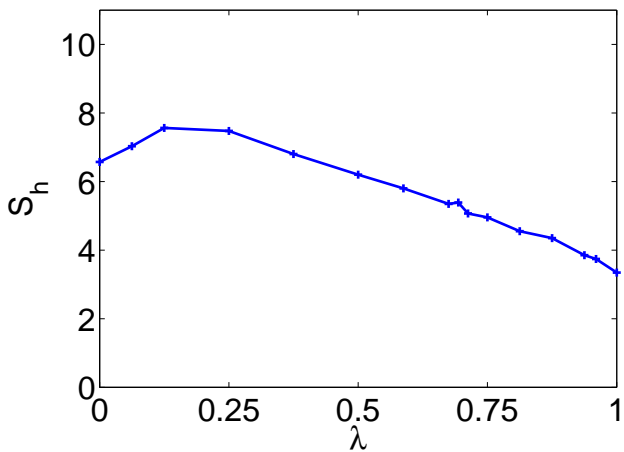
ilar to Fig. 9 and Fig. 10 will be very valuable for reservoir management and risk mitigation. A closed-loop reservoir management system, should compute MV optimal control solutions for $\lambda \in [0, 1]$. This would give the expected NPV, the NPV standard deviation, the Sharpe ratio, and the efficient frontier in a risk-return diagram. The range of possible NPVs are subsequently computed by simulating each of the optimal control solutions for each of the permeability fields in the ensemble. Reservoir engineers and managers could then analyze the diagrams as well as selected bhp trajectories. Based on this analysis, they should select a mean-variance trade-off parameter, λ . This could be the market solution, but it could also be another value. A set of optimal injector and producer well bhp trajectories corresponds to the selected value of λ . The bhp values in the first control period are implemented in the reservoir. Test Case II demonstrated the importance of feedback. To incorporate measurements obtained one control period later, a history



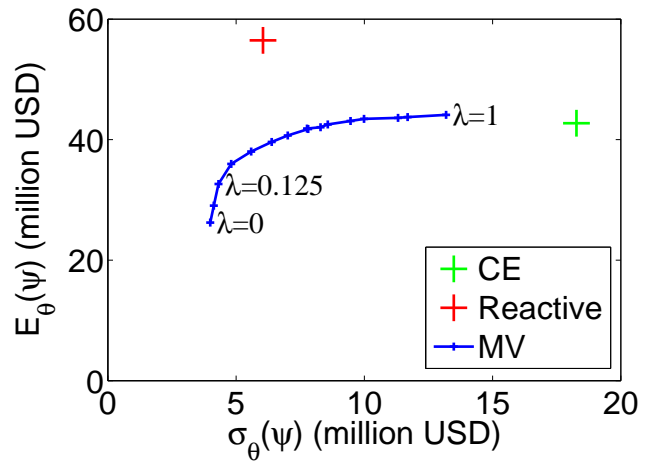
(a) Expected profit, max profit, and min profit.



(b) Risk measured as the standard deviation of profit.



(c) The Sharpe ratio.



(d) A risk-return plot. The expected NPV vs standard deviation of NPV.

Figure 10: Mean-variance relations for Test Case II. Profit (a), risk (b), and Sharpe Ratio (c) for different mean-variance trade-offs, λ . (d) is a phase plot of expected profit vs risk measured as the standard deviation of profit. The blue curve is the efficient frontier. Also the CE and reactive strategy are indicated.

matching procedure should be used to update the ensemble of permeability fields. Based on this updated ensemble of permeability fields, the mean-variance open-loop optimal control computations are repeated and the first part of the selected optimal bhps are implemented (Capolei et al., 2013).

When comparing the efficient frontiers in Fig. 9d and Fig. 10d, it is apparent that the efficient frontier in Fig. 10d is a textbook example of an efficient frontier that is monotonously increasing while the efficient frontier in Fig. 9d is not monotonously increasing. When the efficient frontier is monotonously increasing, increased risk results in increased expected profit. The efficient frontier in Fig. 9d may result from the fact that Test Case I is complicated, but it may also be an artificial result stemming from convergence of the numerical optimization algorithm to different local optima when changing the value of λ .

In the analysis and discussion of the performance of different

control strategies, worst case analysis is beneficial and informative. In this study, we analyzed worst case performance by simulation using a bhp trajectory obtained by open-loop MV optimization; i.e. as part of solving the mean-variance optimal control problem, we computed the NPV, ψ^i , for each member of the ensemble, and the set $\{\psi^i\}_{i=1}^{n_d}$ was used to determine $\psi_{\min} = \min \{\psi^i\}_{i=1}^{n_d}$ and $\psi_{\max} = \max \{\psi^i\}_{i=1}^{n_d}$. In a future study, it would be interesting to compare the MV solution to a max-min solution, i.e. to compute the optimal control trajectories by solution of

$$\max_{\{u_k\}_{k=0}^{N-1}} \min_{i \in \{1, 2, \dots, n_d\}} \psi = \psi(\{u_k\}_{k=0}^{N-1}; x_0, \theta^i) \quad (28a)$$

$$s.t. \quad c(\{u_k\}_{k=0}^{N-1}) \leq 0 \quad (28b)$$

Subsequently, KPIs such as the mean, the standard deviation, and the Sharpe ratio may be computed. These KPIs can be used

Table 3: Key Performance Indicators (KPIs) for Test Case II. The economic KPIs are the expected profit, the standard deviation of the profit, the Sharpe ratio, and the minimum and maximum profit for the ensemble. The reported production related KPIs are the expected oil production, the expected water injection, and the production efficiency, ξ . The productions are normalized by the pore volume. All improvements are relative to the reactive strategy.

Strategy	$\hat{\psi}$		σ		S_h	ψ_{\min}		ψ_{\max}		$E_o[Q_o]$		$E_o[Q_{w.inj}]$		ξ
	10 ⁶ USD, %	%	10 ⁶ USD, %	%		10 ⁶ USD, %	%	10 ⁶ USD, %	%	, %	, %	, %	, %	
Reactive	56.47,	/	6.05,	/	9.33	43.92,	/	70.104,	/	0.35,	/	0.86,	/	39.5
CE	42.72,	-24.35	18.27,	+202.0	2.34	-38.40,	-187.4	72.21,	+3.01	0.26,	-26.0	0.64,	-27.4	40.3
MV														
$\lambda = 1$ (RO)	44.11,	-21.9	13.19,	+118.0	3.34	9.28,	-78.9	67.14,	-4.2	0.23,	-34.9	0.47,	-45.8	47.5
$\lambda = 0.75$	42.52,	-24.7	8.58,	+41.8	4.96	17.93,	-59.2	59.16,	+15.6	0.19,	-44.9	0.33,	-61.9	57.2
$\lambda = 0.5$	39.62,	-29.8	6.39,	+5.6	6.20	21.24,	-51.6	51.82,	-26.1	0.17,	-52.0	0.26,	-70.6	64.6
$\lambda = 0.25$	35.97,	-36.3	4.81,	-20.5	7.48	22.46,	-48.9	46.45,	-33.7	0.15,	-58.0	0.21,	-76.3	70.0
$\lambda = 0.125$	32.64,	-42.2	4.32,	-28.7	7.56	21.29,	-51.5	42.46,	-39.4	0.13,	-62.5	0.18,	-79.6	72.7
$\lambda = 0$	26.23,	-53.5	3.99,	-34.0	6.57	17.37,	-60.5	36.38,	-48.1	0.10,	-71.2	0.12,	-86.1	81.9

to evaluate and compare the max-min solution to the mean-variance solutions.

6. Conclusions

In this paper, we describe a mean-variance approach to risk mitigation in production optimization by open-loop optimal control. The mean-variance approach to risk mitigation is well known in finance and design optimization, but have to our knowledge not been used previously for production optimization of oil reservoirs. By simulation, we demonstrate a computationally tractable method for mean-variance optimal control calculations of a reservoir model consisting of an ensemble of permeability fields. Compared to the RO strategy and the CE strategy, the MV strategy based on the market value of the mean-variance trade-off parameter, λ , is able to reduce risk significantly. This comes at the price of slightly reduced mean profits. In Test Case II, we indicated the importance of feedback. Therefore, future studies should investigate the mean-variance optimal control strategy in a moving horizon closed-loop fashion. Implemented in closed-loop using the moving horizon principle, the optimal control problem for production optimization of an oil reservoir is an example of an Economic Nonlinear Model Predictive Controller (Economic NMPC). We believe that the mean-variance objective function introduced in this paper will be of interest to not only production optimization for closed-loop reservoir management but also for Economic NMPC in general. In the future, the mean-variance approach for production optimization should be compared to other methods for stochastic optimization, e.g. conditional-value-at-risk and two-stage stochastic programming, as well as the modified MV strategy that can shut in uneconomical wells (Capolei et al., 2013).

Acknowledgements

This research project is financially supported by 1) the Danish Research Council for Technology and Production Sciences, FTP Grant no. 274-06-0284; 2) The Danish Advanced Technology Foundation in the OPTION Project (J.nr 63-2013-3); and 3)

the Center for Integrated Operations in the Petroleum Industry at NTNU.

Appendix A. Computation of the MV Objective and its Gradients

The mean-variance objective function for an ensemble is defined as

$$\psi_{MV} = \lambda \hat{\psi} - (1 - \lambda) \sigma^2 \quad (\text{A.1})$$

with the mean and variances computed by

$$\hat{\psi} = \frac{1}{n_d} \sum_{i=1}^{n_d} \psi^i \quad (\text{A.2a})$$

$$\sigma^2 = \frac{1}{n_d - 1} \sum_{i=1}^{n_d} (\psi^i - \hat{\psi})^2 \quad (\text{A.2b})$$

The gradient, $\nabla_{u_k} \psi_{MV}$ for $k \in \mathcal{N}$, is computed as

$$\nabla_{u_k} \psi_{MV} = \lambda \nabla_{u_k} \hat{\psi} - (1 - \lambda) \nabla_{u_k} \sigma^2 \quad k \in \mathcal{N} \quad (\text{A.3})$$

with the gradient of the mean, $\nabla_{u_k} \hat{\psi}$, computed as

$$\nabla_{u_k} \hat{\psi} = \frac{1}{n_d} \sum_{k=1}^{n_d} \nabla_{u_k} \psi^i \quad (\text{A.4})$$

The gradient of the variance, $\nabla_{u_k} \sigma^2$, is

$$\begin{aligned} \nabla_{u_k} \sigma^2 &= \frac{1}{n_d - 1} \sum_{i=1}^{n_d} \left[\nabla_{u_k} (\psi^i - \hat{\psi})^2 \right] \\ &= \frac{2}{n_d - 1} \sum_{i=1}^{n_d} \left[(\psi^i - \hat{\psi}) \nabla_{u_k} (\psi^i - \hat{\psi}) \right] \\ &= \frac{2}{n_d - 1} \sum_{i=1}^{n_d} \left[(\psi^i - \hat{\psi}) (\nabla_{u_k} \psi^i - \nabla_{u_k} \hat{\psi}) \right] \end{aligned} \quad (\text{A.5})$$

$\nabla_{u_k} \sigma^2$ can be computed by (A.5). To compute $\nabla_{u_k} \sigma^2$ more efficiently, we express $\nabla_{u_k} \sigma^2$ as

$$\nabla_{u_k} \sigma^2 = \frac{2}{n_d - 1} \left(\sum_{i=1}^{n_d} \left[(\psi^i - \hat{\psi}) \nabla_{u_k} \psi^i \right] - \sum_{i=1}^{n_d} \left[(\psi^i - \hat{\psi}) \nabla_{u_k} \hat{\psi} \right] \right) \quad (\text{A.6})$$

and note that

$$\begin{aligned} \sum_{i=1}^{n_d} ((\psi^i - \hat{\psi}) \nabla_{u_k} \hat{\psi}) &= \left(\sum_{i=1}^{n_d} (\psi^i - \hat{\psi}) \right) \nabla_{u_k} \hat{\psi} \\ &= \underbrace{\left(\sum_{i=1}^{n_d} \psi^i - n_d \hat{\psi} \right)}_{=0} \nabla_{u_k} \hat{\psi} = 0 \end{aligned}$$

Consequently, the gradient of the variance can be computed efficiently by

$$\nabla_{u_k} \sigma^2 = \frac{2}{n_d - 1} \sum_{i=1}^{n_d} (\psi^i - \hat{\psi}) \nabla_{u_k} \psi^i \quad (\text{A.7})$$

References

- Alhuthali, A.H., Datta-Gupta, A., Yuen, B., Fontanilla, J.P.. Optimal rate control under geologic uncertainty. In: SPE/DOE Symposium on Improved Oil Recovery. Tulsa, Oklahoma, USA; volume 3; 2008. p. 1066–1090. SPE-113628-MS.
- Bertsekas, D.. Dynamic Programming and Optimal Control. Volume 1. 3rd ed. Belmont, Massachusetts: Athena Scientific, 2005.
- Beyer, H.G., Sendhoff, B.. Robust optimization - a comprehensive survey. *Computer Methods in Applied Mechanics and Engineering* 2007;196:3190–3218.
- Biegler, L.T.. Solution of dynamic optimization problems by successive quadratic programming and orthogonal collocation. *Computers and Chemical Engineering* 1984;8:243–248.
- Biegler, L.T.. A survey on sensitivity-based nonlinear model predictive control. In: 10th IFAC International Symposium on Dynamics and Control of Process Systems. Mumbai, India; 2013. p. 499–510.
- Binder, T., Blank, L., Bock, H.G., Burlisch, R., Dahmen, W., Diehl, M., Kroneder, T., Marquardt, W., Schlöder, J.P., von Stryk, O.. Introduction to model based optimization of chemical processes on moving horizons. In: Grötschel, M., Krumke, S., Rambau, J., editors. *Online Optimization of Large Scale Systems*. Berlin: Springer; 2001. p. 296–339.
- Bock, H.G., Plitt, K.J.. A multiple shooting algorithm for direct solution of optimal control problems. In: *Proceedings 9th IFAC World Congress Budapest*. Pergamon Press; 1984. p. 243–247.
- Brouwer, D.R., Jansen, J.D.. Dynamic optimization of waterflooding with smart wells using optimal control theory. *SPE Journal* 2004;9(4):391–402. SPE-78278-PA.
- Capolei, A., Jørgensen, J.B.. Solution of constrained optimal control problems using multiple shooting and ESDIRK methods. In: 2012 American Control Conference. 2012. p. 295–300.
- Capolei, A., Stenby, E.H., Jørgensen, J.B.. High order adjoint derivatives using esdirk methods for oil reservoir production optimization. In: EC-MOR XIII, 13th European Conference on the Mathematics of Oil Recovery. 2012a. .
- Capolei, A., Suwartadi, E., Foss, B., Jørgensen, J.B.. Waterflooding optimization in uncertain geological scenarios. *Computational Geosciences* 2013;17(6):991–1013.
- Capolei, A., Völcker, C., Frydendall, J., Jørgensen, J.B.. Oil reservoir production optimization using single shooting and ESDIRK methods. In: *Proceedings of the 2012 IFAC Workshop on Automatic Control in Offshore Oil and Gas Production*. Trondheim, Norway; 2012b. p. 286–291.
- Chen, Z.. *Reservoir Simulation. Mathematical Techniques in Oil Recovery*. Philadelphia, USA: SIAM, 2007.
- Chierici, G.L.. Economically improving oil recovery by advanced reservoir management. *Journal of Petroleum Science and Engineering* 1992;8(3):205–219.
- Foss, B.. Process control in conventional oil and gas fields - Challenges and opportunities. *Control Engineering Practice* 2012;20:1058–1064.
- Foss, B., Jensen, J.P.. Performance analysis for closed-loop reservoir management. *SPE Journal* 2011;16(1):183–190. SPE-138891-PA.
- Hansen, P.C.. *Rank-Deficient and Discrete II-Posed Problems: Numerical Aspects of Linear Inversion*. SIAM, Philadelphia, 1998.
- Heirung, T.A.N., Wartmann, M.R., Jansen, J.D., Ydstie, B.E., Foss, B.A.. Optimization of the water-flooding process in a small 2d horizontal oil reservoir by direct transcription. In: *Proceedings of the 18th IFAC World Congress*. 2011. p. 10863–10868.
- Jansen, J.. Adjoint-based optimization of multi-phase flow through porous media - A review. *Computers & Fluids* 2011;46:40–51.
- Jansen, J.D., Bosgra, O.H., Van den Hof, P.M.J.. Model-based control of multiphase flow in subsurface oil reservoirs. *Journal of Process Control* 2008;18:846–855.
- Jansen, J.D., Douma, S.D., Brouwer, D.R., Van den Hof, P.M.J., Bosgra, O.H., Heemink, A.W.. Closed-loop reservoir management. In: 2009 SPE Reservoir Simulation Symposium. The Woodlands, Texas, USA; 2009. p. 856–873. SPE 119098-MS.
- Jørgensen, J.B.. Adjoint sensitivity results for predictive control, state- and parameter-estimation with nonlinear models. In: *Proceedings of the European Control Conference 2007*. Kos, Greece; 2007. p. 3649–3656.
- Lazarov, B., Schevenels, M., Sigmund, O.. Topology optimization with geometric uncertainties by perturbation techniques. *International Journal for Numerical Methods in Engineering* 2012;90(11):1321–1336.
- Lie, K.A., Krogstad, S., Ligaarden, I.S., Natvig, J.R., Nilsen, H.M., Skaflestad, B.. Open source matlab implementation of consistent discretisations on complex grids. *Computational Geosciences* 2012;16(2):297–322.
- Liu, Y.. Using the snesim program for multiple-point statistical simulation. *Computers & Geosciences* 2006;32(10):1544–1563.
- Markowitz, H.. Portfolio selection. *The Journal of Finance* 1952;7(1):77–91.
- MATLAB, . version 7.13.0.564 (R2011b). Natick, Massachusetts: The Math-Works Inc., 2011.
- Nævdal, G., Brouwer, D.R., Jansen, J.D.. Waterflooding using closed-loop control. *Computational Geosciences* 2006;10:37–60.
- Peaceman, D.W.. Interpretation of well-block pressures in numerical reservoir simulation with nonsquare grid blocks and anisotropic permeability. *SPE Journal* 1983;23:531–543.
- Ramirez, W.F.. *Application of Optimal Control Theory to Enhanced Oil Recovery*. Elsevier Science Ltd, 1987.
- Sarma, P., Aziz, K., Durlofsky, L.J.. Implementation of adjoint solution for optimal control of smart wells. In: *SPE Reservoir Simulation Symposium*, 31 January-2 February 2005, The Woodlands, Texas. 2005a. p. 67–83.
- Sarma, P., Durlofsky, L., Aziz, K.. Efficient closed-loop production optimization under uncertainty. In: *SPE Europepec/EAGE Annual Conference*. Madrid, Spain; 2005b. p. 583–596.
- Schlegel, M., Stockmann, K., Binder, T., Marquardt, W.. Dynamic optimization using adaptive control vector parameterization. *Computers and Chemical Engineering* 2005;29:1731–1751.
- Schölkopf, B., Smola, A., Müller, K.R.. Nonlinear component analysis as a kernel eigenvalue problem. *Neural Computation* 1998;10(5):1299–1319.
- Sharpe, W.F.. The sharpe ratio. *The Journal of Portfolio Management* 1994;21(1):49–58.
- Steinbach, M.C.. Markowitz revisited: Mean-variance models in financial portfolio analysis. *SIAM Review* 2001;43(1):31–85.
- Stengel, R.F.. *Optimal Control and Estimation*. New York: Dover Publications, 1994.
- Suwartadi, E., Krogstad, S., Foss, B.. Nonlinear output constraints handling for production optimization of oil reservoirs. *Computational Geosciences* 2012;16:499–517.
- Van Essen, G.M., Van den Hof, P.M.J., Jansen, J.D.. Hierarchical long-term and short-term production optimization. *SPE Journal* 2011;16(1):191–199. SPE-124332-PA.
- Van Essen, G.M., Zandvliet, M.J., Van den Hof, P.M.J., Bosgra, O.H., Jansen, J.D.. Robust waterflooding optimization of multiple geological scenarios. *SPE Journal* 2009;14(1):202–210. SPE-102913-PA.
- Völcker, C., Jørgensen, J.B., Stenby, E.H.. Oil reservoir production optimization using optimal control. In: 50th IEEE Conference on Decision and Control and European Control Conference. Orlando, Florida; 2011. p. 7937–7943.
- Völcker, C., Jørgensen, J.B., Thomsen, P.G., Stenby, E.H.. Simulation of subsurface two-phase flow in an oil reservoir. In: *Proceedings of the European Control Conference 2009*. Budapest, Hungary; 2009. p. 1221–1226.
- Yasari, E., Pishvaie, M.R., Khorasheh, F., Salahshoor, K., Kharrat, R.. Application of multi-criterion robust optimization in water-flooding of oil reservoir. *Journal of Petroleum Science and Engineering* 2013;109:1–11.